Molecular Crystals and Liquid Crystals
Publication details, including instructions for authors and subscription information:
http://www.tandfonline.com/loi/gmcl16

Analysis of Electric Field Induced Deformations in a Nematic Liquid Crystal for any Applied Field

K. R. Welford [a] & J. R. Sambles [a]
[a] Department of Physics, University of Exeter, Exeter, Devon, U.K., EX4 4QL
Version of record first published: 28 Mar 2007.

To cite this article: K. R. Welford & J. R. Sambles (1987): Analysis of Electric Field Induced Deformations in a Nematic Liquid Crystal for any Applied Field, Molecular Crystals and Liquid Crystals, 147:1, 25-42

To link to this article: http://dx.doi.org/10.1080/00268948708084622

Mol. Cryst. Liq. Cryst., 1987, Vol. 147, pp. 25–42
Photocopying permitted by license only

Printed in the United States of America

Analysis of Electric Field Induced Deformations in a Nematic Liquid Crystal for any Applied Field

K. R. WELFORD and J. R. SAMBLES
Department of Physics, University of Exeter, Exeter, Devon, U.K. EX4 4QL

(*Received August 7, 1986*)

For the first time, expressions are presented which enable us to calculate the reorientation of the nematic director under the influence of an applied voltage of any magnitude. The mathematical techniques developed are extended to study the capacitance of a nematic layer under any magnitude of applied voltage. The calculation of the capacitance of the nematic layer up to high applied voltages allows the identification of a new high voltage linear relationship between capacitance and applied voltage. This new linear relationship has potential for enabling the anisotropic dielectric permittivity of liquid crystal materials to be measured experimentally with more accuracy and ease than before.

Keywords: nematic liquid crystals, electric field deformations

INTRODUCTION

The nematic liquid crystal phase is an anisotropic fluid which exhibits a degree of orientational order. Average molecular orientation within the bulk fluid is described by the director, the orientation of which, in general, varies from point to point within the bulk fluid but may be persuaded to align uniformly between two bounding surfaces. The properties of this aligned layer are then highly anisotropic. Of particular interest in this work, is the anisotropic dielectric constant of the material, which has uniaxial symmetry. If the nematic layer is placed in an applied electric field the director will be induced to reorientate *via* the interaction between the anisotropic dielectric con-

Anyone requiring listing of the FORTRAN programs used please contact the authors.

stant and the applied field. The reorientation of the director causes modifications to the electrical and optical properties of the layer. These changes are of major importance to the applications of nematic materials in electro-optic displays. In order to be able to achieve accurate modelling of liquid crystal display devices it is not only necessary to be able to calculate the director configuration in the nematic layer under the influence of an applied field but also to know the magnitudes of the dielectric anisotropy, the optical anisotropy and the elastic anisotropy.

If the capacitance and optical birefringence of a uniformly aligned layer are monitored as a function of an applied electric field experimental measurements may be made that allow the anisotropies of the nematic material to be deduced. Many studies of this kind have been made, see e.g. Ohtsu *et al.*,[1] Gruler *et al.*[2]). To interpret the experimental data and deduce the dielectric, optical, and elastic anisotropies we need to be able to calculate the behaviour of the nematic director under the influence of the applied electric field. The standard analysis procedure is provided by Deuling[3] and involves a calculation of the minimum energy configuration in the applied field. Deuling's innovative work allows this minimization procedure to be performed for any magnitude of anisotropy, but is of limited scope in that direct calculation of the director profile at large applied voltage is not possible using his analytic expressions. The correlation of experimental data with the theoretical model for small applied fields is less satisfactory than for large fields. This has led workers such as Meyerhofer[4] and Clark *et al.*[5] to seek a high field asymptotic forms of the nematic capacitance and Balzarini *et al.*[6] to seek high field asymptotic form of the nematic optical birefringence. At the present time it is possible to model the aligned nematic layer accurately at the low and high applied electric field limits but not over all voltages.

This work demonstrates how Deuling's analysis can be extended to allow the director profile, and hence the capacitance to be computed at any voltage.

BASIC MODEL

Consider a parallel aligned homogeneous nematic liquid crystal cell in which a cartesian coordinate system is chosen such that the direction normal to the bounding plane surfaces is the z direction and with no applied voltage, the director lies along the x direction. Thus the director remains perpendicular to the y direction regardless of the applied voltage. The dielectric constant perpendicular to the director

is denoted ϵ_n and the dielectric constant parallel to the director is ϵ_p. When a voltage V is applied across the cell, if $\epsilon_p > \epsilon_n$, provided V is above a certain threshold voltage V_0 the liquid crystal undergoes an elastic deformation. The director then tilts with respect to the x axis, the amount of tilt ϕ being a function of the distance from the aligning surfaces. Deuling[3] considered the case of strong anchoring at the boundaries and considered, for all voltages the tilt at these boundaries, $z = 0$ and $z = L$, remains equal to zero, i.e. $\phi(0) = 0 = \phi(L)$. For the sake of simplicity, we shall adopt the same boundary conditions although it is not particularly difficult to generalise the equations developed to the case of finite tilt at the boundaries provided one retains strong anchoring. It is however, somewhat more difficult to evaluate the equations for weak coupling and the implications for this case are currently being pursued.

Deuling's[3] approach involves minimizing the Gibbs free energy G, per unit area of the system

$$G = \int_0^L [F_{el} + F_{diel}]\, dz \tag{1}$$

where F_{el} is the free energy per unit volume due to elastic deformation and F_{diel} is the free energy per unit volume associated with the applied electric field. By application of continuum elasticity theory (see e.g. Frank[7]) to the nematic liquid crystal director geometry it is simple to show that

$$F_{el} = \frac{1}{2}\left(\frac{d\phi}{dz}\right)^2 (k_{11}\cos^2\phi + k_{33}\sin^2\phi) \tag{2}$$

while the form for F_{diel} may be established from elementary electrostatics and is found to be

$$F_{diel} = -\frac{1}{2}\epsilon_0 E^2 (\epsilon_p \sin^2\phi + \epsilon_n \cos^2\phi) \tag{3}$$

Applying the calculus of variations to find the function $\phi(z)$ which minimizes the integral (1), Deuling showed that for the boundary conditions $\phi(0) = 0 = \phi(L)$

$$\frac{V}{V_0} = \frac{2}{\pi}(1 + \gamma\sin^2\phi_m)^{1/2} \int_0^{\phi_m} \left[\frac{1 + k\sin^2\phi}{(1 + \gamma\sin^2\phi)(\sin^2\phi_m - \sin^2\phi)}\right]^{1/2} d\phi \tag{4}$$

and

$$\frac{2z}{L}\int_0^{\phi m}\left[\frac{(1+k\sin^2\phi)(1+\gamma\sin^2\phi)}{\sin^2\phi_m-\sin^2\phi}\right]^{1/2}d\phi$$

$$=\int_0^{\phi}\left[\frac{(1+k\sin^2\phi)(1+\gamma\sin^2\phi)}{\sin^2\phi_m-\sin^2\phi}\right]^{1/2}d\phi \quad (5)$$

where V_0 is the threshold voltage given by

$$V_0=\pi\left[\frac{k_{11}}{\epsilon_0(\epsilon_p-\epsilon_n)}\right]^{1/2}$$

$$\gamma=\frac{\epsilon_p-\epsilon_n}{\epsilon_n},\ k=\frac{k_{33}-k_{11}}{k_{11}}$$

and ϕ_m is the maximum tilt angle, which by symmetry occurs at the middle of the cell, $\phi_m=\phi(L/2)$.

In principle we can use equation (4) in an iterative fashion to evaluate ϕ_m for a given applied voltage V. From this value of ϕ_m one may then evaluate the complete tilt profile using equation (5). However a mathemetical difficulty appears in the integrands because of the factor $(\sin^2\phi_m-\sin^2\phi)$ in the denominators. As ϕ approaches ϕ_m this factor creates an infinite singularity in the integrand. To avoid this problem Deuling[3] proposed a straightforward change of variables by substituting

$$\sin\phi=\sin\phi_m.\sin\psi$$

and

$$\eta=\sin^2\phi_m$$

leading to

$$\frac{V}{V_0}=\frac{2}{\pi}(1+\gamma\eta)^{1/2}\int_0^{\pi/2}\left[\frac{1+\kappa\eta\sin^2\psi}{(1+\gamma\eta\sin^2\psi)(1-\eta\sin^2\psi)}\right]^{1/2}d\psi \quad (6)$$

and

$$\frac{2z}{L}\int_0^{\pi/2}\left[\frac{(1+\kappa\eta\sin^2\psi)(1+\gamma\eta\sin^2\psi)}{1-\eta\sin^2\psi}\right]^{1/2}d\psi$$

$$=\int_0^{\sin^{-1}(\sin\phi/\eta^{1/2})}\left[\frac{(1+\kappa\eta\sin^2\psi)(1+\gamma\eta\sin^2\psi)}{1-\eta\sin^2\psi}\right]d\psi \qquad (7)$$

These integrals, which are readily evaluated using standard numerical computational techniques, may be conveniently used for any values of z and ψ provided η is not very close to 1. Clearly as η approaches 1 (that is ϕ_m approaches $\pi/2$) once again infinities appear in the integrals because of the $(1-\eta\sin^2\psi)$ factor in the denominator. Unfortunately on evaluation of equation (6) it is soon found that ϕ_m converges rapidly to $\pi/2$ for $V/V_0 > 4$. Thus in order to evaluate $\phi(z)$ for $V/V_0 > 4$ it is essential that ϕ_m is known very precisely to avoid the infinity. In practice calculated tilt profiles show errors at $V/V_0 \sim 3$ unless double precision routines are utilised and the integrals broken up into a large number of regions. Using such an approach we have been able to extend these calculations up to $V/V_0 \sim 15$. However this is a very unwieldy and time consuming approach and clearly it would be better to evolve a technique which would overcome the reliance upon an accurately known ϕ_m.

THE NEW APPROACH

The simplest way to avoid precision problems with ϕ_m is to perform the calculations using $\tan\phi_m$, or for mathematical simplicity $\tan^2\phi_m$. As V/V_0 increases then while ϕ_m rapidly converges to $\pi/2$, $\tan^2\phi_m$ is steadily increasing towards infinity. This is apparent from Figures 1a and 1b where we show ϕ_m and $\log(\tan^2\phi_m)$ as functions of the normalized voltage V/V_0 for a sample with parameters as listed in Table I. Particularly striking is the linear dependence of $\log(\tan^2\phi_m)$ on V/V_0 for $V/V_0 \geq 4$, and we shall return to this later. For the moment we shall concentrate on evaluating the integrals with the following substitutions in equations (6) and (7):

$$Y = \tan^2\phi_m = \frac{\eta}{1-\eta}$$

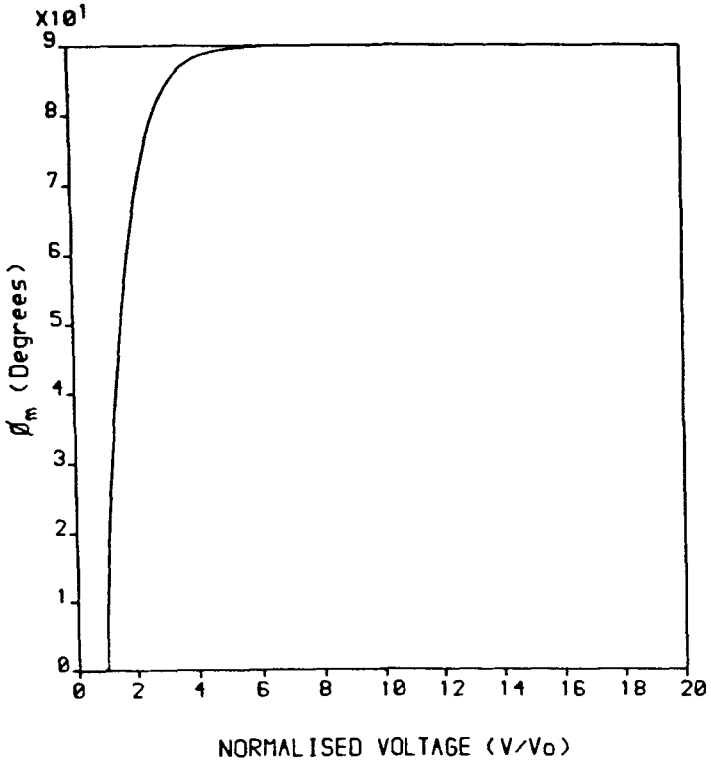

(a)

FIGURE 1 The maximum director tilt, ϕ_m as a function of the normalised voltage V/V_0.
(a) Linear plot of ϕ_m against V/V_0 (b) Plot of $\log(\tan^2\phi_m)$ against V/V_0

and $W = \tan^2\psi$. Thus we find

$$\frac{V}{V_0} = \frac{1}{\pi}(1 + Y(1+\gamma))^{1/2} \int_0^\infty \cdot \left[\frac{(1+Y)(1+W) + \kappa YW}{[(1+Y)(1+W) + \gamma YW](1+Y+W)(1+W)W}\right]^{1/2} dW \qquad (8)$$

and

$$\frac{2z}{L}\int_0^\infty \left[\frac{[(1+Y)(1+W)+\kappa YW][(1+Y)(1+W)+\gamma YW]}{(1+Y+W)(1+Y)(1+W)W}\right]^{1/2} \frac{dW}{1+W}$$

$$= \int_0^{W_l} \left[\frac{[(1+Y)(1+W)+\kappa YW][(1+Y)(1+W)+\gamma YW]}{(1+Y+W)(1+Y)(1+W)W}\right]^{1/2} \frac{dW}{1+W} \qquad (9)$$

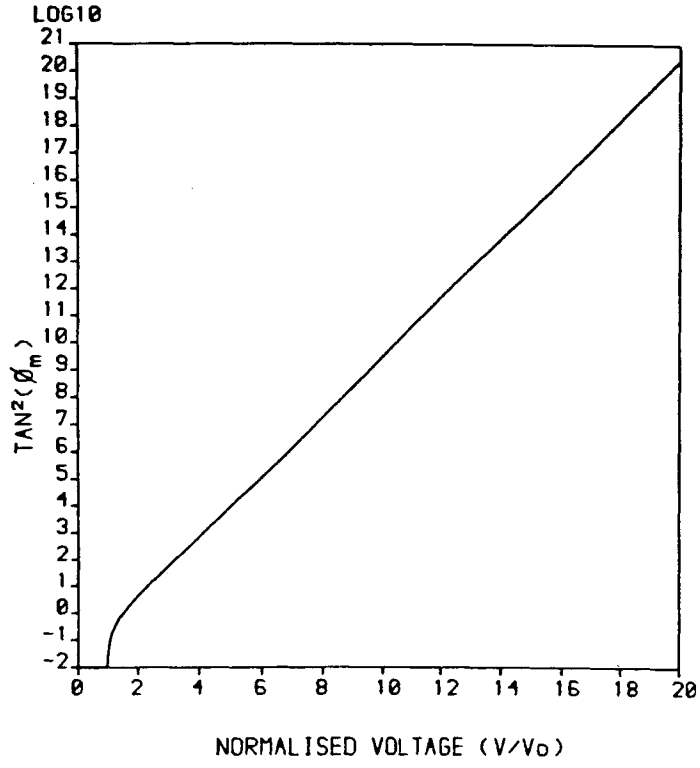

(b)

Figure 1 (*continued*)

where W_l, the upper limit in the last integral is given by

$$W_l = \frac{\sin^2\phi}{\sin^2\phi_m - \sin^2\phi} = \frac{\tan^2\phi(1 + Y)}{Y - \tan^2\phi}$$

TABLE I

Parameters for the liquid crystal modelled in the calculations presented in this paper

Parameter	Symbol	Value
Extraordinary refractive index	n_e	1.737
Ordinary refractive index	n_0	1.518
Parallel relative permittivity	ϵ_p	20.25
Perpendicular relative permittivity	ϵ_n	5.355
Splay elastic constant	K_{11}	1.113×10^{-11} N
Bend elastic constant	K_{33}	1.7129×10^{-11} N
Layer thickness	L	10 μm
Wavelength of incident radiation	λ	632.8×10^{-9}m

All the integrals in equations (8) and (9) are readily evaluated using numerical integration routines specifically designed to deal with the infinities in the upper limits. It is from such integration routines that we obtain Figures 1a, 1b and 2. In Figure 2 we show the tilt profile as a function of V/V_0 also for the material parameters of Table I. Note in these three Figures the ability to compute the response at voltages far in excess of V_0.

Thus we see that this simple substitution allows computation of the tilt profiles for any experimentally reasonable voltages. However these new equations are not particularly useful for analytic examination of the high voltage limit behaviour and yet it is clear from Figure 1b that simple analytic expressions should be found in this limit. Essentially, one has to find a second method for dealing with the infinities in the denominators of the integrands. Returning to equation (6) it is apparent that another way of handling the problem is to rewrite

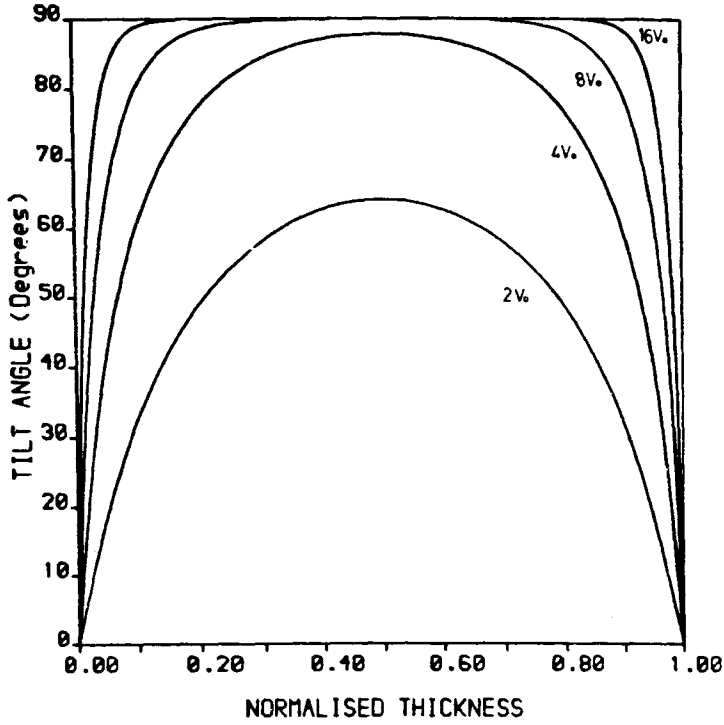

FIGURE 2 Tilt angle ϕ as a function of normalised distance, z/L, through the cell for various normalised voltages V/V_0.

the equation as follows:

$$\frac{V}{V_0} = \frac{2}{\pi}(1 + \gamma\eta)^{1/2} \int_0^{\pi/2} \left[\left(\frac{1 + \kappa\eta\sin^2\psi}{1 + \gamma\eta\sin^2\psi} \right)^{1/2} - \left(\frac{1 + \kappa\eta}{1 + \gamma\eta} \right)^{1/2} \right] \frac{d\psi}{(1 - \eta\sin^2\psi)^{1/2}} + \frac{2}{\pi}(1 + \kappa\eta)^{1/2} \int_0^{\pi/2} \frac{d\psi}{(1 - \eta\sin^2\psi)^{1/2}} \quad (10)$$

Both of these integrals are now well behaved in the limit $\eta \to 1$, that is high voltages. The first integral is merely a constant, C_0 (for $\eta \to 1$) which may be readily evaluated by computer using the substitutions introduced above. The second integral may be found in tables of complete elliptic integrals and in the limit $\eta \to 1$ gives

$$\int_0^{\pi/2} \frac{d\psi}{(1 - \eta\sin^2\psi)^{1/2}} \to \frac{1}{2} \ln \left(\frac{16}{1 - \eta} \right) = \frac{1}{2} \ln (1 + Y) + \ln 4$$

or in the limit Y ($= \tan^2\phi_m$) tending to infinity this becomes simply

$$\frac{1}{2}\ln(\tan^2\phi_m) + \ln 4.$$

Hence equation (10) gives

$$\lim_{V >> V_0} \frac{V}{V_0} = \frac{2}{\pi}(1 + \kappa)^{1/2} \left[\frac{1}{2} \ln \left(\tan^2\phi_m \right) + \ln 4 \right] + \frac{2}{\pi}(1 + \kappa)^{1/2} C_0 \quad (11)$$

where C_0 is a numerical constant which depends on γ and κ.

Hence we see at high voltages there is a simple linear relationship between V/V_0 and $\log(\tan^2\phi_m)$ as shown from our numerical calculations in Figure 1b, the gradient of this graph is just $\pi \log e/(1 + \kappa)^{1/2}$. This then provides a check on our evaluation of ϕ_m, but in order to check our computation of tilt profiles it was felt expedient to examine also $d\phi/dz|_{z=0 \text{ or } L}$ in this high voltage limit, thus ascertaining behaviour both at the edges and in the middle of

the cell. From Deuling[3] we have

$$\frac{d\phi}{dz} = D_z \left(\frac{\gamma}{\epsilon_0 \epsilon_n k_{11}}\right)^{1/2} \left[\frac{\sin^2\phi_m - \sin^2\phi}{(1 + \kappa\sin^2\phi)(1 + \gamma\sin^2\phi)(1 + \gamma\sin^2\phi_m)}\right]^{1/2} \tag{12}$$

where

$$D_z = \frac{2}{L}\left[\frac{\epsilon_0\epsilon_n k_{11}}{\gamma}\right]^{1/2}\left[1 + \gamma\sin^2\phi_m\right]^{1/2} \cdot \int_0^{\phi_m}\left[\frac{(1 + \kappa\sin^2\phi)(1 + \gamma\sin^2\phi)}{\sin^2\phi_m - \sin^2\phi}\right]^{1/2} d\phi \tag{13}$$

giving thus at $z = 0$, when $\phi = 0$

$$\left.\frac{d\phi}{dz}\right|_0 = \frac{2}{L}\sin\phi_m \int_0^{\phi_m}\left[\frac{(1 + \kappa\sin^2\phi)(1 + \gamma\sin^2\phi)}{\sin^2\phi_m - \sin^2\phi}\right]^{1/2} d\phi \tag{14}$$

This expression may be readily transformed to a numerically integratable form by making the previous two step substitution into one using

$$\sin^2\phi_m = \frac{Y}{1 + Y} = \eta$$

and

$$\sin^2\phi = \left(\frac{Y}{1 + Y}\right)\left(\frac{W}{1 + W}\right)$$

giving

$$L\left.\frac{d\phi}{dz}\right|_0 = \left(\frac{Y}{1+Y}\right)^{1/2} \cdot \int_0^{\infty}\left[\frac{[(1 + Y)(1 + W) + \kappa YW][(1 + Y)(1 + W) + \gamma YW]}{(1 + Y + W)(1 + Y)(1 + W)W}\right]^{1/2} \frac{dW}{1+W} \tag{15}$$

which may be evaluated numerically giving for the parameters of

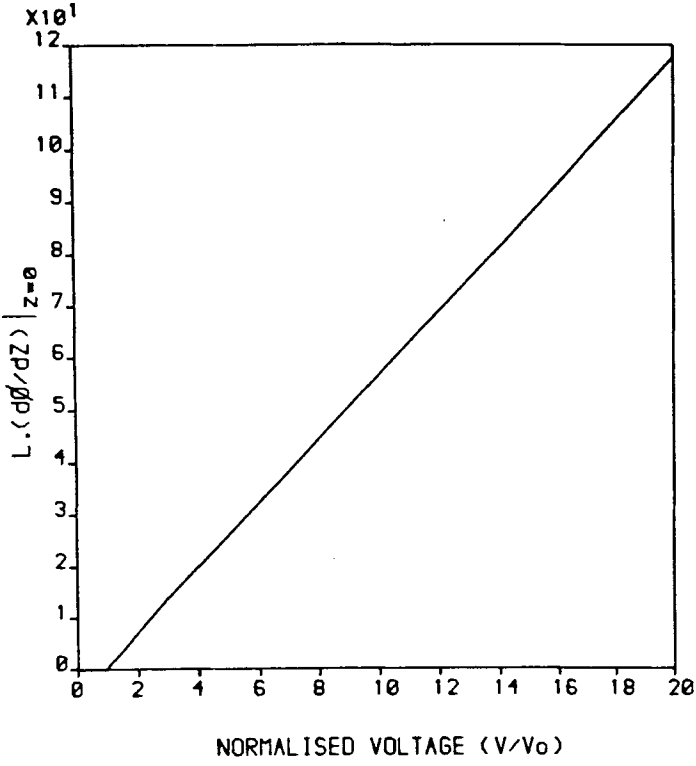

FIGURE 3 Plot of the normalized gradient of the tilt angle at the cell $L\, d\phi/dz|_0$, against normalised voltage V/V_0.

Table I the V/V_0 dependence shown in Figure 3. Here again an obvious linear dependence of $d\phi/dz|_0$ with V/V_0 is seen for $V/V_0 \geqslant 3$. This prompts us therefore to rewrite equation (14), using Deulings substitution, and then regrouping the integrand to give:

$$L\left.\frac{d\phi}{dz}\right|_0 = 2\eta^{1/2}\int_0^{\pi/2}\frac{[(1+\kappa\eta\sin^2\psi)(1+\gamma\eta\sin^2\psi)]^{1/2}-[(1+\kappa\eta)(1+\kappa\eta)]^{1/2}}{(1-\eta\sin^2\psi)^{1/2}}d\psi + 2\eta^{1/2}\int_0^{\pi/2}\left[\frac{(1+\kappa\eta)(1+\gamma\eta)}{1-\eta\sin^2\psi}\right]^{1/2}d\psi \qquad (16)$$

where we again avoid the infinity in the integrand in the first integral.

If we now combine equations (16) and (10) we find after rearranging

$$L\left.\frac{d\phi}{dz}\right|_0 = \pi\eta^{1/2}(1+\gamma\eta)^{1/2}\frac{V}{V_0} - 2\gamma\eta^{3/2}\int_0^{\pi/2}\frac{\cos^2\psi(1+\kappa\eta\sin^2\psi)^{1/2}}{[(1+\gamma\eta\sin^2\psi)(1-\eta\sin^2\psi)]^{1/2}}\,d\psi$$

which in the limit $\eta \to 1$ becomes

$$\lim_{V>>V_0} L\frac{d\phi}{dz} = \pi(1+\gamma)^{1/2}\frac{V}{V_0} - 2\gamma\int_0^{\pi/2}\left(\frac{1+\kappa\sin^2\psi}{1+\gamma\sin^2\psi}\right)^{1/2}\cos\psi\,d\psi \qquad (17)$$

which gives directly the linear dependance of $d\phi/dz|_0$ upon V/V_0 for $V/V_0 \geqslant 2$.

The integral in (17) may be re-expressed as

$$I(17) = \int_0^1 \frac{dx}{[(1+\kappa x^2)(1+\gamma x^2)]^{1/2}} + \kappa\int_0^1 \frac{x^2dx}{[(1+\kappa x^2)(1+\gamma x^2)]^{1/2}}$$

which are two elliptic integrals, again found in standard tables, see for example Gradshtyn and Ryzhik[8] p. 245 (3.152:1) and p. 246 (3.153:1). We write

$$\int_0^1 \frac{dx}{[(1+\kappa x^2)(1+\gamma x^2)]^{1/2}} = \frac{1}{\sqrt{\kappa\gamma}}\int_0^1 \frac{dx}{[(a^2+x^2)(b^2+x^2)]^{1/2}}$$

where $a^2 = 1/\kappa$, $b^2 = 1/\gamma$ $(a > b)$ and

$$\int_0^1 \frac{x^2dx}{[(1+\kappa x^2)(1+\gamma x^2)]^{1/2}} = \frac{1}{\sqrt{\kappa\gamma}}\int_0^1 \frac{dx}{[(a^2+x^2)(b^2+x^2)]^{1/2}}$$

giving

$$I(17) = \frac{1}{\sqrt{\kappa\gamma}}\frac{1}{a}F(\alpha,q) + \frac{\kappa}{\sqrt{\kappa\gamma}}\left[\left(\frac{a^2+1}{b^2+1}\right)^{1/2} - aE(\alpha,q)\right]$$

where

$$\alpha = \arctan\left(\frac{1}{b}\right), \quad q = \frac{(a^2 - b^2)^{1/2}}{a}$$

and F is an elliptic integral of the first kind, E an elliptic integral of the second kind.

$$\mathrm{I}(17) = \left(\frac{1 + \kappa}{1 + \gamma}\right)^{1/2} + \frac{1}{\sqrt{\gamma}}\{F(\alpha,q) - E(\alpha,q)\}$$

with

$$\alpha = \arctan(\gamma^{1/2}) \quad \text{and} \quad q = \left(\frac{\gamma - \kappa}{\gamma}\right)^{1/2}$$

This allows (17) to be finally expressed as

$$\begin{aligned} \underset{V/V_0 \geq 3}{\text{Limit}}\, L\left.\frac{d\phi}{dz}\right|_0 &= \pi(1 + \gamma)^{1/2}\frac{V}{V_0} - 2\gamma\left(\frac{1 + \kappa}{1 + \gamma}\right)^{1/2} \\ &\quad - 2\gamma^{1/2}\{F(\alpha,q) - E(\alpha,q)\} \qquad (18) \\ &= \pi(1 + \gamma)^{1/2}\frac{V}{V_0} + 2C_1 \end{aligned}$$

This simple linear dependence confirms the numerical calculations and also suggests that further important parameters for liquid crystal cells may be examined in the same manner. One of the more commonly measured cell parameters is the capacitance and it is to this we now turn our attention.

CAPACITANCE

The capacitance per unit area of the cell may be shown to be[2]

$$C = \frac{\epsilon_0\epsilon_n}{L}\frac{\displaystyle\int_0^{\phi_m}\left[\frac{(1 + \kappa\sin^2\phi)(1 + \gamma\sin^2\phi)}{\sin^2\phi_m - \sin^2\phi}\right]^{1/2} d\phi}{\displaystyle\int_0^{\phi_m}\left[\frac{1 + \kappa\sin^2\phi}{(1 + \gamma\sin^2\phi)(\sin^2\phi_m - \sin^2\phi)}\right]^{1/2} d\phi} \qquad (19)$$

in which there are again divergence problems with both integrals. Making the transformations to W and Y introduced above, (19) becomes

$$C = \frac{\epsilon_0 \epsilon_n}{L} \frac{\int_0^\infty \left\{ \frac{[(1+Y)(1+W)+\kappa YW][(1+Y)(1+W)+\gamma YW]}{(1+Y+W)(1+Y)(1+W)W} \right\}^{1/2} \frac{dW}{(1+W)}}{\int_0^\infty \left\{ \frac{[(1+Y)(1+W)+\kappa YW](1+Y)}{[(1+Y)(1+W)+\gamma YW](1+Y+W)(1+W)W} \right\}^{1/2} dW} \tag{20}$$

which as before is now readily evaluated by numerical techniques up to high voltages giving the C against V/V_0 dependence displayed in Figure 4a.

Inspection of equation (19) reveals that there is no need to go through the above integration procedure, since the numerator is effectively given by equation (14) and the denominator by equation (4). Thus

$$C = \frac{\epsilon_0 \epsilon_n}{L} \frac{\frac{L}{2\sin\phi_m} \left.\frac{d\phi}{dz}\right|_0}{\frac{V}{V_0} \frac{\pi}{2[1+\gamma\sin^2\phi_m]^{1/2}}} = \frac{\epsilon_0 \epsilon_n}{\pi} \frac{V_0}{V} \left[\frac{1+\gamma\sin^2\phi_m}{\sin^2\phi_m} \right]^{1/2} \left.\frac{d\phi}{dz}\right|_0 \tag{21}$$

However equation (18) gives the limit expression for

$$L \left.\frac{d\phi}{dz}\right|_0 \qquad \text{for } V >> V_0,$$

and thus with $\sin\phi_m \to 1$

$$\lim_{V>>V_0} C = \frac{\epsilon_0 \epsilon_n}{L\pi} (1+\gamma)^{1/2} \cdot \frac{V_0}{V} \left[\pi(1+\gamma)^{1/2} \frac{V}{V_0} - 2\gamma \left[\frac{1+\kappa}{1+\gamma} \right]^{1/2} - 2\gamma^{1/2} \{F(\alpha,q) - E(\alpha,q)\} \right]$$

or

$$\frac{LC}{\epsilon_0\epsilon_n(1+\gamma)}\frac{V}{V_0} = \frac{V}{V_0} - \frac{2\gamma}{\pi}\frac{(1+\kappa)^{1/2}}{1+\gamma} - \frac{2}{\pi}\left(\frac{\gamma}{1+\gamma}\right)^{1/2}\{F(\alpha,q) - E(\alpha,q)\}$$

which with $C_\infty = \epsilon_0\epsilon_n/L\,(1+\gamma) = \epsilon_0\epsilon_p/L$ gives

$$\begin{aligned}&\lim_{V>>V_0} C\frac{V}{V_0}\\ &= C_\infty\frac{V}{V_0} - \frac{2C_\infty}{\pi}\left[\frac{\gamma(1+\kappa)^{1/2}}{1+\gamma} + \left(\frac{\gamma}{1+\gamma}\right)^{1/2}\{F(\alpha,q) - E(\alpha,q)\}\right]\\ &= C_\infty\frac{V}{V_0} + \frac{2C_\infty}{(1+\gamma)^{1/2}\pi}C_1 \qquad (22)\end{aligned}$$

This predicts that a graph of CV/V_0 against V/V_0 becomes a straight line with slope given by C_∞ at the high voltage limit. Such a dependence is clearly illustrated in Figure 4b which is obtained by numerical integration of (20). It is interesting to note how well the linear dependence is obeyed. This accords well with the asymptotic limit of Clark *et al.*[5] They showed that, in this limit, C is proportional to $1/V$ which in our case follows directly from (22). We illustrate this type of plot in Figure 4c. However, while these two types of plot are almost the same, it would appear from the large range of linearity in Figure 4b that equation (22) remains a good approximation even for relatively low voltages. As an illustration of this, we differentiate (22) with respect to V/V_0 and thereby examine the slope as a function of V/V_0 as shown in Figure 4d. Remarkably, we find that this graph has an "overshoot" causing the high voltage gradient C_∞ to be reached by $4V_0$. This thus provides experimentalists with a rapid procedure for measuring C_∞ and hence ϵ_p, without approximation.

CONCLUSIONS

We have developed a general approach which allows the evaluation of the response of a homogeneously aligned liquid crystal cell at any

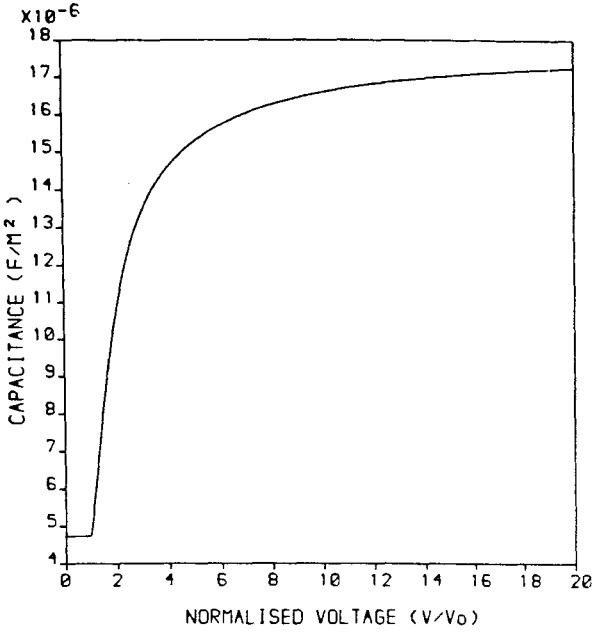

(a)

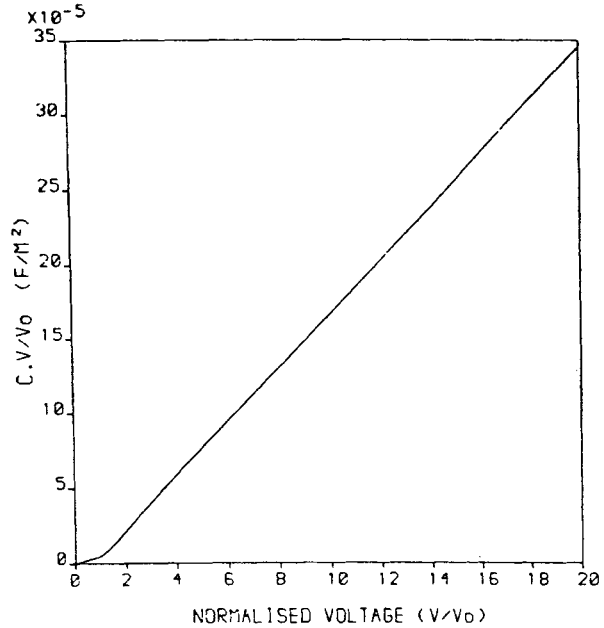

(b)

FIGURE 4 The variation of capacitance, C, with the normalised voltage V/V_0.
(a) Plot of C versus V/V_0 (b) Plot of CV/V_0 versus V/V_0
(c) Plot of C versus V_0/V (d) Plot of $d(CV/V_0)/d(V/V_0)$ against V/V_0

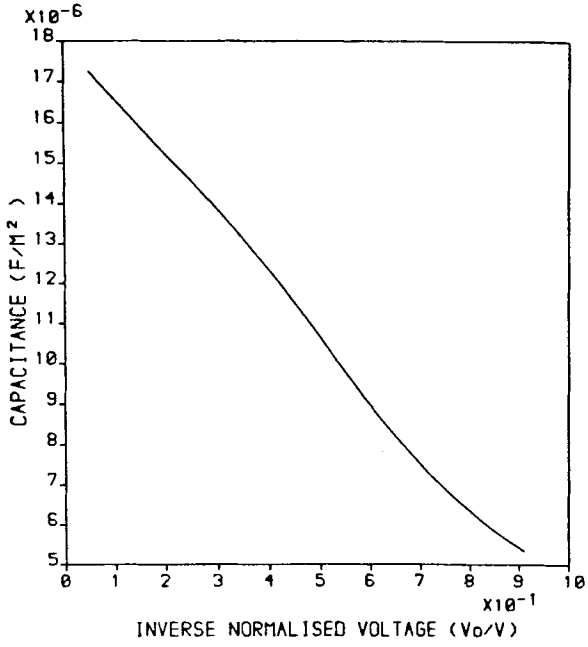

(c)

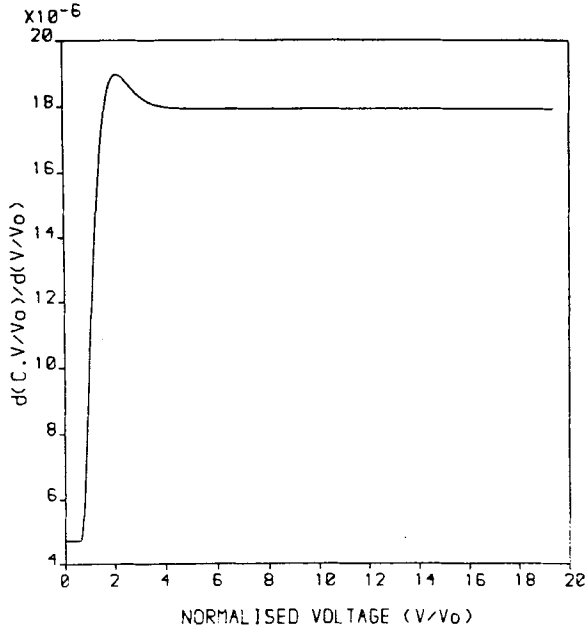

(d)

Figure 4 (*continued*)

voltage. The form of the high voltage response for such a cell has also been examined and analytic forms obtained which lend themselves to experimental verification. It has been shown how at high voltages, greater than a few times the threshold voltage, there is a simple linear dependence of capacitance times voltage upon voltage. Further it is clear that from this dependence it is a simple matter to obtain the dielectric constants of the liquid crystal under study. Applying the mathematical techniques to an analysis of the optical birefringence also leads to a simple linear dependence. An example of this type of analysis can be found in Balzarini *et al.*[6] The mathematical procedures developed here are currently being extended to other interesting cases, in particular finite surface tilt, homeotropic alignment and the influence of magnetic fields are being examined.

Acknowledgments

The authors wish to thank Dr. M. Clark for his help at the beginning of this work, Dr. K. Harrison for supplying information on E7 and his continuous support and Dr. T. W. Preist for help with the integration techniques. KRW also acknowledges the support of an SERC CASE award in collaboration with RSRE Malvern.

References

1. M. Ohtsu, T. Akahane and T. Tako, *Japanese Journal of Applied Physics*, **13**, 4, 621 (1974).
2. H. Gruler, T. J. Scheffer and G. Meier, *Z. Naturforsch*, **27** A, 966 (1972).
3. H. J. Deuling *Mol. Cryst. Liq. Cryst.*, **19**, 123 (1972).
4. D. Meyerhofer, *Mol. Cryst. Liq. Cryst.*, **34**, 13 (1976).
5. M. G. Clark, E. P. Raynes, R. A. Smith and R. J. A. Tough, *J. Phys. D: Appl. Phys.*, **13**, 2154 (1980).
6. D. A. Balzarini, D. A. Dunmur and P. Palffy-Muhoray, *Mol. Cryst. Liq. Cryst.*, **102**, 35 (1984).
7. F. C. Frank, *Disc. Farad. Soc.*, **25**, 19 (1958).
8. I. S. Gradshtyn and I. M. Ryzhik, "Tables of Integrals, Series and Products." Academic Press (1980).